ACS OMEGA

Open Access

http://pubs.acs.org/journal/acsodf

Article

Poly(styrene-*alt*-maleic acid)-assisted Membrane Solubilization for Improved Immobilization and Catalytic Performance of Soybean Lipolytic Enzymes in Electrospun Poly(vinyl alcohol) Fibers

Kamonchanok Thananukul, Patnarin Worajittiphon, Kitiphong Khongphinitbunjong, Orawan Suwantong, Sittiruk Roytrakul, Siripat Aluksanasuwan, Matthew J. Derry, Paul D. Topham, and Patchara Punyamoonwongsa*

Cite This: *ACS Omega* 2026, 11, 5608−5621

Read Online

ACCESS | Metrics & More | Article Recommendations | Supporting Information

ABSTRACT: Efficient extraction and stabilization of plant-derived enzymes remain challenging due to their susceptibility to denaturation during processing. Soybean lipases, while exhibiting intrinsically high activity, lose functionality rapidly in the presence of salts, organic solvents, or elevated temperatures, thereby limiting their direct industrial use. To address these challenges, we developed a poly(styrene-*alt*-maleic acid) (PSMA)-assisted extraction and immobilization platform that simultaneously disrupts membranes and forms stable catalytic nanoparticles suitable for nanofiber fabrication. When applied to *Glycine max* (soybean) extracts, the PSMA-assisted process yielded the highest specific lipase activity of 16 mU/mg under optimized conditions (pH 7.5; mass-to-buffer volume ratio 1:25). Proteomic profiling identified 16 proteins showing significant abundance differences between conventional MOPS-buffered and PSMA/MOPS-assisted extractions, confirming selective stabilization of lipolytic enzymes. Morphological characterization revealed that the immobilized enzymes self-assembled into spherical, homogeneous nanoparticles with an average diameter of 227 nm. Incorporating 1% (w/v) of these nanoparticles into electrospun poly(vinyl alcohol) (PVA) fibers enhanced the enzyme activity by nearly 3-fold relative to the prespun solution, while maintaining comparable fiber size to the unloaded membranes (174 ± 65 nm vs 138 ± 31 nm, $p > 0.05$). By integrating the self-assembly behavior of PSMA with electrospun PVA nanofibers, this work demonstrates a scalable and effective route for preserving enzymatic function and fabricating ultrafine catalytic membranes for industrial biocatalysis.

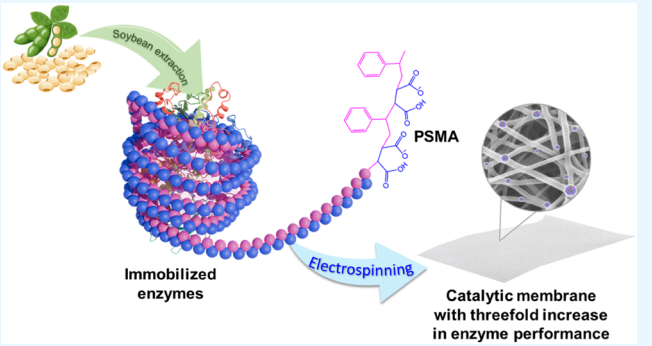

1. INTRODUCTION

Plant-derived proteins, including enzymes, have been extensively extracted and purified for diverse applications, such as proteomic analysis, dietary supplementation, and industrial biocatalysis. Among these, lipolytic enzymes, particularly esterases and lipases, are of considerable industrial value due to their roles in biorefineries, pharmaceuticals, and food processing, with the global enzyme market projected to reach USD 14.5 billion by 2027.[1] In plants, lipases catalyze the hydrolysis of storage triacylglycerols into alcohols and free fatty acids, which are subsequently metabolized to support seedling growth.[2] Soybean lipases, in particular, exhibit relatively high activity (10.4 mU/mL/min) but are prone to activity loss upon exposure to ionic salts,[3] organic solvents, or elevated temperatures,[4] limiting their direct use in industrial applications.

To overcome these limitations, immobilization strategies have been widely explored to enhance enzyme stability and reusability. Physical adsorption onto polymer matrices maintains structural integrity but suffers from enzyme leaching and chemical degradation. Covalent attachment provides stronger binding effects,[3,5] but can lead to conformational changes that reduce catalytic activity.[6,7] Entrapment within polymeric networks offers a gentler alternative. This approach provides a combined sieving and shielding effect that minimizes leakage while preserving enzymatic activity.[8−11] Electrospinning technology has emerged as a promising entrapment method, producing nanofibrous membranes with exceptionally high surface-to-volume ratios, tunable porosity, and enhanced mass transfer, thereby improving catalytic efficiency and enantioselectivity over conventional immobiliza-

Received: September 6, 2025
Revised: October 25, 2025
Accepted: January 9, 2026
Published: January 21, 2026

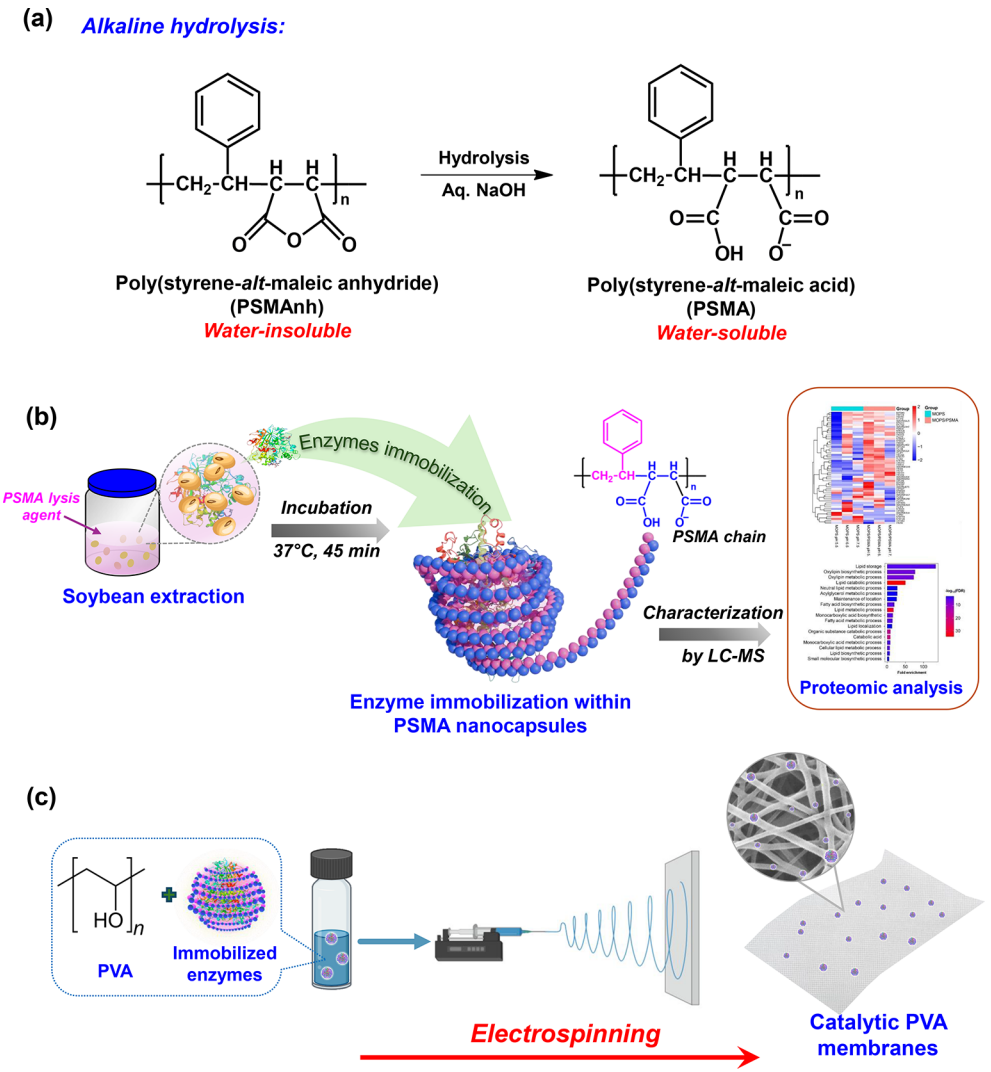

Figure 1. Illustrations of: (a) alkaline hydrolysis of PSMAnh producing water-soluble PSMA, (b) direct extraction and immobilization of soybean enzymes into PSMA nanocapsules (hydrophobic styrene groups shown in pink and carboxyl groups shown in blue), with the extracted biomolecules, depicted in multicolor curled ribbons, analyzed for proteomic patterns using LC−MS technique, and (c) electrospinning of immobilized enzymes with poly(vinyl alcohol) (PVA, 10% w/v), producing catalytic PVA fibrous membranes.

tion.[12−17] In electrospinning, the target enzyme is physically blended with the polymer solution. Under an applied electric field, the solution forms an elongated conical structure, known as a Taylor cone, at the spinneret tip. Once electrostatic forces overcome the surface tension of a droplet, a polymer jet is ejected, stretched, and solidified via solvent evaporation, yielding ultrafine nanofibers. Adjusting electrospinning parameters, such as applied voltage, feed composition, and working distance, allows precise control over fiber diameter and morphology. Despite these advantages, electrospinning can induce protein denaturation due to high electric fields, mechanical stresses, dehydration, solvent exposure, and localized heating.[5,18,19] To reduce these effects, strategies such as coaxial or emulsion electrospinning,[20] stabilizer addition,[21,22] use of aqueous/green solvents,[23] and nanoencapsulation[24,25] have been proposed. Among these, nanoencapsulation is especially promising, as it provides a protective shell that shields enzymes from harsh processing conditions while maintaining their native conformation and activity. For instance, β-glucuronidase encapsulated in liposomes prior to electrospinning retained longer-term activity compared to the free-enzyme approach.[24] Another study reported a near-complete activity of bovine carbonic anhydrase (BCA) when protected by zeolite imidazolate framework (ZIF-8) carriers within poly(vinyl alcohol) (PVA) electrospun fibers.[26]

Our previous work demonstrated a one-step, entirely aqueous poly(styrene-*alt*-maleic acid) (PSMA)-assisted extraction and nanoencapsulation of soybean lipolytic enzymes.[27] This method reduces processing time, solvent consumption, and operational costs compared to conventional multistep purification, while minimizing protein denaturation from organic solvent exposure, pH shifts, and temperature fluctuations. PSMA is usually obtained via alkaline hydrolysis of the PSMAnh precursor (Figure 1a). It disrupts and completely destabilizes biological membranes above its critical aggregation concentration (> 0.1% w/v), enabling the release of cytoplasmic components into the surrounding medium.[28] Under these conditions, PSMA molecules can also self-assemble into nanostructures, wherein the aromatic rings form a nonpolar core, while maleic acid groups form a corona in the aqueous phase. This nanostructure creates a protective

https://doi.org/10.1021/acsomega.5c09274
ACS Omega 2026, 11, 5608−5621

microenvironment for encapsulated enzymes (Figure 1b). Using this approach, we previously achieved a 2-fold increase in specific lipolytic activity (2.0 U/mg) compared to free-enzymes.[27]

While several studies have demonstrated the use of PSMA for extraction and immobilization, most of them focused on synthetic model compounds[29−33] or transmembrane proteins[34−36] rather than complex plant-derived systems. Earlier PSMA-assisted extraction studies, including our prior work,[27] provided only a proof-of-concept evidence without addressing how factors such as solution pH and a soybean mass-to-buffer volume ratio (m/v) influence polymer ionization state,[37,38] self-assembly, and membrane interaction. In this study, we systematically optimized PSMA-assisted extraction of soybean lipolytic enzymes under varied pH and m/v ratio conditions, followed by proteomic characterization using liquid chromatography−mass spectrometry (LC−MS). The resulting enzyme-PSMA complexes were subsequently incorporated into electrospun poly(vinyl alcohol) (PVA) nanofibers (Figure 1c), selected for their hydrophilicity, biocompatibility, biodegradability, and fiber-forming ability.[39−42] By integrating PSMA's protective self-assembly with the structural and mass-transfer advantages of electrospun fibrous membranes, this approach minimizes enzyme deactivation during electrospinning and yields a highly active, plant-derived biocatalyst suitable for industrial applications. Notably, this work provides the first systematic and proteomic-level insight into PSMA-assisted extraction and immobilization, bridging polymer chemistry with enzymology for future scalable biocatalysis.

2. MATERIALS AND METHODS

2.1. Materials

Soybeans (*Glycine max*) were purchased from a local market in Chiang Rai Province, Thailand. Poly(styrene-*alt*-maleic anhydride) (PSMAnh) was obtained from Sartomer (USA), possessing a 1:1 copolymer composition and a number-average molecular weight (M_n) of 1.5 × 10^3 g/mol.[27] 4-Morpholinepropanesulfonic acid (MOPS) and 4-nitrophenyl butyrate (pNPB) were purchased from Sigma-Aldrich, USA. Both dithiothreitol (DTT) and Pierce bicinchoninic acid (BCA) agents were purchased from Thermo Scientific, USA. Sulfuric acid (98%, AR grade) and ethanol (99.9%, AR grade) were supplied from QRëC, Malaysia. Poly(vinyl alcohol) (PVA, Mowiol 18-88) with a degree of hydrolysis of 86−89% and a molecular weight (M_w) of 1.3 x 10^5 g/mol was obtained from Sigma-Aldrich, Germany. Aqueous solutions of hydrochloric acid (HCl, 1.0 N) and sodium hydroxide (NaOH, 1.0 N) were obtained from KemAus, Australia. A commercial wheat germ lipase (Type I, lyophilized powder, 5−15 units/mg) was obtained from Sigma-Aldrich, USA. All chemicals were used as received without further purification.

2.2. Preparation of Water-soluble PSMA

Under constant stirring conditions, 1 g of PSMAnh was dissolved in 100 mL of Milli-Q water. The pH of the solution was adjusted to 12 by adding NaOH solution. Once a clear solution was obtained, it was neutralized by adding HCl and precipitated in chilled acetone (5-fold excess). The solid residue (PSMA) was washed with a minimum of cold water and finally dried to a constant weight in a vacuum oven at 60 °C.

2.3. Extraction of Soybean Seeds

A lysis buffer, containing MOPS (0.1 M), DTT (1 mM), and PSMA (1% w/v), was prepared in Milli-Q water. The addition of DTT served to prevent protein precipitation, while its concentration was carefully limited to 1 mM to minimize potential interference in subsequent colorimetric assays. The pH buffer was adjusted to 5.5, 6.5, and 7.5 by adding either HCl or NaOH. For the extraction, an appropriate amount of soybean seeds was preconditioned by soaking in Milli-Q water at 25 °C for 24 h. The dehulling and cracking were performed using a kitchen blender (11,000 rpm for 3 min). Subsequently, 25 mL of the lysis buffer was added, and the slurry was incubated on an orbital shaker at 37 °C for 45 min. After incubation, the mixture was centrifuged at 9,000 rpm for 20 min at 4 °C. The supernatant was collected and freeze-dried into powder under vacuum (1.05 × 10^{-5} MPa).

2.4. Characterization of Soybean Extracts

Dynamic light scattering (DLS; Malvern, Zetasizer Nano ZS) was used to determine the mean particle size and size distribution of the crude enzyme extracts. Before measurement, the freeze-dried sample was redissolved in Milli-Q water to a final concentration of 1% (w/v). The solution was sonicated at a low amplitude (15%) for 20 min and stirred continuously for 24 h at room temperature. All measurements were performed at 25 °C. Average particle sizes were calculated from three replicates and reported as mean ± standard deviation (SD). Scanning electron microscopy (SEM, Tescan MIRA) was used to observe the morphology of the enzyme particles. For this analysis, the freeze-dried powder was redissolved in Milli-Q water to a final concentration of 0.1% (w/v). The solution was stirred at 150 rpm for 24 h at room temperature. A 25 μL aliquot was then dropped onto carbon tape mounted on an SEM stub and dried at 60 °C for 8 h. Images were acquired by using an accelerating voltage of 15 kV and a working distance of 10 mm.

The total protein content and lipase activity were measured to evaluate the specific lipase activity of the freshly derived extract solutions and the redissolved aqueous solutions of - freeze-dried crude extracts (or electrospun membranes). Total protein concentration was determined using the bicinchoninic acid (BCA) assay (Thermo Fisher Scientific), which was selected for its tolerance to reducing agents, such as 1 mM DTT. A series of bovine serum albumin (BSA) standards (62.5−1,000 μg/mL) was prepared in Milli-Q water. For the assay, 10 μL of either the BSA standards or extracted solution was mixed with 300 μL of the working reagent in a 96-well plate. The plate was incubated at 37 °C for 30 min before measuring the light absorbance at 562 nm by using a microplate reader. To minimize matrix effects from PSMA or DTT, all samples were diluted at least 10-fold in Milli-Q water, and a buffer-only blank was used as a background control. All measurements were performed in triplicate, and the protein content was reported as mean ± SD.

Lipase activity was determined by using *p*-nitrophenyl butyrate (pNPB) as a substrate. A 10 mM pNPB solution was prepared in deionized water and diluted at a volume ratio of 1:99 (pNPB/water). The solution pH was adjusted to 7.5 by using potassium phosphate buffer to obtain the final substrate solution. For the assay, 0.9 mL of the substrate solution was mixed with 0.1 mL of the extracted solution and incubated at 37 °C for 60 min. The reaction was terminated by adding 2 mL of absolute ethanol. Enzymatic activity was determined by measuring the light absorbance at 405 nm, corresponding to the release of *p*-nitrophenol (pNP). One unit of enzyme activity (U) was defined as the amount of enzyme that releases 1 μmol of pNP per minute under the assay conditions. The activity was calculated using the equation: $A = \varepsilon lC$, where A is absorbance, ε is the molar extinction coefficient (1.457 × 10^5 cm^2/mol), l is the optical path length (1 cm), and C is the molar concentration, respectively.[43] Specific lipase activity was reported as U/mg of total protein. All data were expressed as the mean ± standard deviation (SD) of triplicate measurements.

2.5. Protein Analysis

Protein concentration for LC−MS-based proteomic analysis was determined using the modified Lowry assay with BSA as a protein standard.[44] The upstream SDS-PAGE workflow inherently removes interfering compounds, such as PSMA, which is critical for efficient in-gel digestion and successful LC−MS analysis. Briefly, a standard curve plot was generated by plotting the optical density at 750 nm (OD_{750}) of the BSA solutions against their concentrations (μg/mL). This standard curve was used to calculate the protein concentration in the crude extracts. For protein fractionation, an SDS-PAGE mini slab gel

https://doi.org/10.1021/acsomega.5c09274
ACS Omega 2026, 11, 5608−5621

(8 cm × 9 cm × 0.1 cm; Hoefer miniVE, Amersham Biosciences, UK) was prepared at 12.5% acrylamide following the standard method described by Laemmli.[45] Equal volumes of the protein samples were mixed with 5 μL of 5X loading buffer (0.125 M Tris-HCl at pH 6.8, 20% glycerol, 5% SDS, 0.2 M DTT, 0.02% bromophenol blue). The mixture was heated at 95 °C for 10 min before loading onto 12.5% SDS-PAGE. To estimate the molecular weights of the polypeptides, a low molecular weight protein standard marker (Amersham Biosciences, UK) was used. Electrophoresis was performed in the running buffer (25 mM Tris-HCl pH 8.3, 192 mM glycine, and 0.1% SDS) until the tracking dye reached the bottom of the gel. After electrophoresis, the gel was silver-stained according to a published protocol.[46]

The protein bands were excised from the gel, and the gel plugs were dehydrated with 100% acetonitrile (ACN) before reacting with 10 mM DTT in 10 mM ammonium bicarbonate at room temperature for 1 h. Alkylation was performed in the dark at room temperature for 1 h using 100 mM iodoacetamide (IAA) in 10 mM ammonium bicarbonate. The gel pieces were subsequently dehydrated twice with 100% ACN for 5 min each. For in-gel protein digestion, 10 μL of trypsin solution (10 ng/μL in 50% ACN/10 mM ammonium bicarbonate) was added to the gels, followed by incubation at room temperature for 20 min. A 20 μL portion of 30% ACN was further added to ensure full submersion during digestion. The gels were incubated overnight at 37 °C. Peptides were extracted by adding 30 μL of 50% ACN in 0.1% formic acid (FA), followed by shaking at room temperature for 10 min. The peptide extracts were collected, transferred to new tubes, dried by using a vacuum centrifuge concentrator, and stored at −80 °C for subsequent mass spectrometric analysis.

The tryptic peptides were analyzed using an Ultimate3000 Nano/Capillary LC System (Thermo Scientific, UK) coupled to a ZenoTOF 7600 mass spectrometer (SCIEX, Framingham, MA, USA). Peptide enrichment was performed on the μ-Precolumn (300 μm inner diameter × 5 mm) packed with PepMap 100 resin (5 μm, 100 Å, Thermo Scientific, UK). Separation was performed using a 75 μm i.d. × 15 cm column packed with Acclaim PepMap RSLC C18 resin (2 μm, 100 Å, nanoViper, Thermo Scientific, UK), housed in a thermostated-HPLC column maintained at 60 °C. Solvent A (0.1% formic acid in water) and solvent B (0.1% formic acid in 80% acetonitrile) were delivered to the analytical column. Peptides were separated using a gradient elution of 5−55% solvent B at a flow rate of 0.30 μL/min over 30 min.

LC−MS analyses were performed in triplicate for each of the two independent biological replicates. Protein quantification was performed using MaxQuant 2.1.4.0 equipped with the Andromeda search engine.[47] MS/MS spectra were searched against the UniProt *Glycine max* database. Label-free quantitation was performed using MaxQuant's parameters as follows: a maximum of two missed cleavages, a mass tolerance of 0.6 Da for the main search, trypsin as the digesting enzyme, carbamidomethylation of cysteine as a fixedmodification, and oxidation of methionine and acetylation of the protein N-terminus as the variable modifications. For protein identification, peptides with a minimum length of 7 amino acids and at least one unique peptide were required. Proteins were identified if they were supported by at least two peptides, one of which was unique. The protein FDR was set at 1% and estimated using reversed search sequences. The maximum number of modifications per peptide was set to 5. The FASTA file used for searching contained the *Glycine max* proteome downloaded from UniProt on 23 November 2023. Statistical differences in protein intensities among the 6 groups were assessed using ANOVA. Comparisons between the MOPS and MOPS/PSMA groups were performed using an unpaired *t* test. Gene Ontology (GO) enrichment analysis was performed using ShinyGO version 0.80.[48]

2.6. Preparation and Characterization of Electrospun Membranes

An aqueous solution of 10% (w/v) PVA was prepared in deionized water at 60 °C. Freeze-dried soybean extract powder was then added to achieve a final concentration of 1%, 2%, or 4% (w/v). To ensure homogeneity, the mixture was stirred (150 rpm) at ambient temperature (20 °C) for 30 min. Electrospinning was performed at 22 ± 1 °C and 45% relative humidity (RH) using parameters as follows: a pumping rate of 0.8 mL/h, 22 kV applied voltage through a direct current (DC) power supplier, and a working distance between the collector and spinneret of 15 cm. The electrospun fibers were collected on an aluminum sheet adhered to the collector. The as-prepared electrospun fibers were stored in a desiccator cabinet (30% RH) prior to analysis. A rotational viscometer (IKA ROTAVISC Io-vi model) with a spindle SP-3 was used to measure the viscosity of the prespun solutions. All measurements were performed at 23 ± 1 °C at a fixed speed of 20 rpm.

To examine fiber size distribution and fiber morphology, the freshly prepared electrospun membranes were air-dried for at least 72 h. The membranes were then cut into 10 mm × 10 mm rectangles and mounted onto SEM stubs. Gold sputtering was performed for 3 min. SEM images were acquired at an accelerating voltage of 15 kV with a working distance of 10 mm. Fiber diameters were analyzed using ImageJ processing software (n = 100).

The specific lipase activity of the catalytic electrospun PVA membranes (with soybean enzymes) was determined using the same protocol as that for the crude enzyme extracts. For both the BSA assay and lipase activity tests, the as-prepared electrospun membranes were redissolved in Milli-Q water and stirred at 150 rpm and room temperature for 24 h prior to measurement. All measurements were performed in triplicate, and the results were expressed as mean ± SD.

The incorporation of enzyme-loaded electrospun PVA membranes was investigated by Fourier transform-infrared (FT-IR) spectroscopy. All FT-IR spectra were collected in attenuated total reflection (ATR) mode on a Nicolet iS5 spectrometer equipped with a diamond ATR accessory. The measurements were conducted at a 2 cm^{-1} resolution with 32 scans.

2.7. Statistical Analysis

Statistical analysis was performed using IBM SPSS Statistics (ver. 26) and GraphPad Prism (version 8.0.1). Data were tested for normality and analyzed using one-way analysis of variance (ANOVA). When significant differences were observed (P < 0.05), Tukey's multiple comparison test was applied. Graphical visualizations were performed by using GraphPad Prism (version 8.0.1) and the SRplot online tool.[49]

3. RESULTS AND DISCUSSION

Aqueous-based extraction of plant bioactive compounds is influenced by several key parameters, including the polarity of the targeted compounds, solution pH, energy inputs, the mass/volume ratio of plant tissue to the lysis buffer, and the presence of surfactants. Once detached from the plant cells, these bioactive compounds must be transferred into a protective reservoir to prevent chemical degradation caused by external stimuli factors such as UV-light, oxygen gas, acidification, alkalinity, and salt ions. For this reason, the current extraction process was limited to 45 min, following the highest catalytic profile of soybean enzymes reported previously.[50,51] The application of poly(styrene-*alt*-maleic acid) (PSMA) as a membrane lysis agent for the extraction of transmembrane proteins has been previously reported.[27,52] The efficiency of PSMA in membrane disruption is primarily governed by its surface affinity, which is significantly influenced by the solution pH. At pH values above its acid dissociation constant (pK_a > 4.0), the carboxylic acid side groups of PSMA are deprotonated, resulting in electrostatic repulsion between carboxylate anions. This repulsion prevails the hydrophobic interactions among the styrene moieties, leading to an extended polymer conformation with relatively low surface activity.[53] In contrast, under acidic conditions (pH ≤ 4.0),

https://doi.org/10.1021/acsomega.5c09274
ACS Omega 2026, 11, 5608−5621

protonation of the carboxyl groups reduces electrostatic repulsion forces, allowing hydrophobic interactions to become a dominant factor. Consequently, the polymer adopts a collapsed chain conformation, which displays enhanced surface activity acquired for membrane destabilization and release of cytoplasmic constituents. While acidification to pH 4 can promote nearly complete membrane destabilization, the use of nonphysiological pH may cause protein denaturation. To balance membrane lysis efficiency with the preserved native protein structure, extraction in this study was conducted within the pH range 5.5−7.5.

Figure 2 presents the specific lipase activity of crude soybean extracts obtained by using PSMA as a membrane lysis agent at

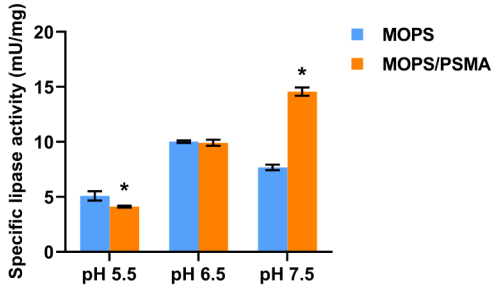

Figure 2. Effect of pH on the specific lipase activity of the freshly derived extract solutions obtained from different buffer treatments. Extraction was performed at 25 °C for 45 min by using a mass-to-volume ratio of 1:12. Blue bars represent crude extracts using the MOPS buffer, while orange bars correspond to those using the MOPS/PSMA buffer. Data are expressed as mean ± SD (n = 3). Asterisks (*) indicate significant differences compared to the MOPS buffer (P < 0.001).

pH 5.5, 6.5, and 7.5. In this assay, ethanol was employed as the quenching agent instead of a conventional sodium carbonate (Na_2CO_3) solution to ensure instantaneous termination of enzyme activity while preserving the physical integrity of the reaction matrix. Strong alkaline quenchers can introduce abrupt pH shifts that promote nonenzymatic hydrolysis of pNPB and rapid precipitation of the final products. In contrast, ethanol provides rapid enzyme denaturation without altering ionic strength or triggering secondary reactions, thereby improving data consistency and reproducibility. Although ethanol alone does not provide alkaline conditions and thus limits the maximum absorbance of p-nitrophenol at 405 nm, the assay still captured a clear trend in the relative lipase activity between the MOPS and MOPS/PSMA treatments. As noticed, the sample treated with the pH 7.5 MOPS/PSMA buffer displayed a significantly higher specific lipase activity than that treated with the pH 7.5 MOPS buffer alone (P < 0.001). The presence of PSMA thus contributed to the enhanced catalytic function, possibly through the formation of a protective reservoir, arising from by a PSMA self-aggregate above its critical aggregation concentration (CAC).[37] In this structure, the hydrophobic styrene moieties are buried within the core, while the hydrophilic maleic acid residues are oriented toward the aqueous surface.[29,54,55] This structural arrangement produces a hydrophobic core capable of entrapping low-to-moderate polarity compounds. Previous studies have demonstrated successful immobilization of various bioactive agents within this PSMA self-assembly, including heme oxygenase inhibitor-zinc protoporphyrin (ZnPP),[29] anticancer temoporfin,[54] antifungal amphotericin B (AmB),[55] propolis,[56] temoporfin,[54] and raloxifene.[31] Taking into consideration that the PSMA concentration used in this study (1 wt %, w/v) was well above the reported CAC, the polymer was expected to exist predominantly in an aggregated state. Consistently, its dynamic light scattering (DLS) profile displayed a monomodal size distribution centered at approximately 18 nm (see Supplementary Figure S1). Once established, this PSMA aggregate can serve as a reservoir for the extracted enzymes to reside in and be shielded from external stimuli factors, therefore avoiding the risk of physicochemical changes and protein denaturation. Among the tested MOPS/PSMA systems, the treatment at pH 7.5 resulted in the highest specific lipase activity. This observation is consistent with a previous report describing alkaline lipases that exhibit maximal catalytic efficiency under mildly alkaline conditions (pH 8.0).[4] The enhanced specific lipase activity observed at pH 7.5 in this study suggests that the catalytic domains of the extracted enzymes remained functionally intact and that the PSMA interaction did not significantly interfere with the native conformation required for effective catalysis. The effect of a soybean mass to buffer volume (m/v) ratio was further demonstrated based on the 45 min extraction time at pH 7.5. The results are presented in Figure 3. As expected,

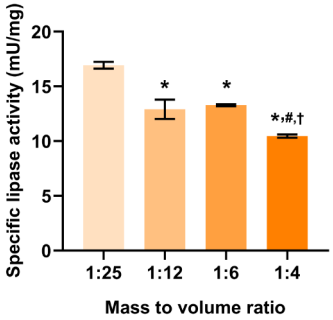

Figure 3. Effect of a soybean mass-to-buffer volume ratio, ranging from 1:25 to 1:4, on the specific lipase activity of the freshly derived extract solutions obtained from different buffer treatments. Extraction was performed in pH 7.5 MOPS/PSMA at 25 °C for 45 min. Data are expressed as mean ± SD (n = 3). Asterisks (*), number sign (#), and dagger (†) indicate statistically significant differences relative to the m/v ratios of 1:25, 1:12, and 1:6, respectively (P < 0.01).

extraction by using the lowest m/v ratio (1:25) exhibited the greatest specific lipase activity (P < 0.01). This is not a surprise since the reduced m/v ratio generally increases the mass transfer of solutes (e.g., PSMA) across the cell membranes, resulting in more efficient PSMA-induced membrane disruption and release of enzymes to the media.

Protein profiling of soybean extracts treated with MOPS buffer and MOPS/PSMA buffer at pH 5.5, 6.5, and 7.5 was performed by using LC−MS analysis. A total of 56 significantly altered proteins were identified across the treatment groups (Supplementary Figure S2 and Table S1). Among these, 16 proteins showed significant differences between the pH 7.5 MOPS buffer and the pH 7.5 MOPS/PSMA buffer treatments (Table 1). The volcano plot and heatmap, illustrating differentially expressed proteins between the two sample groups, are presented in Figure 4a and Figure 4b, respectively. Remarkably, oleosin (I1N747), GDSL esterase/lipase (I1M1M1), and GDSL esterase/lipase APG (I1KGH4) were exclusively identified in the pH 7.5 MOPS/PSMA extracts, as presented in Table 1. Compared to the pH 7.5 MOPS group,

https://doi.org/10.1021/acsomega.5c09274
ACS Omega 2026, 11, 5608−5621

Table 1. List of Significantly Altered Proteins in the Freshly Derived Extract Solutions Treated with pH 7.5 MOPS Buffer or pH 7.5 MOPS/PSMA Buffer

No.	UniProt accession number	Protein name	Mass (kDa)	Intensity (Mean ± SD)		Fold change (Log2)	*P*-value
				MOPS pH 7.5	MOPS/PSMA pH 7.5		
1	I1N747	Oleosin	23589	0 ± 0	8.06 ± 0.21	MOPS/PSMA only	< 0.0001
2	I1M1M1	GDSL esterase/lipase	32594	0 ± 0	6.33 ± 2.12	MOPS/PSMA only	0.0067
3	I1KGH4	GDSL esterase/lipase APG	32102	0 ± 0	8.24 ± 0.18	MOPS/PSMA only	< 0.0001
4	I1KHH3	GDSL esterase/lipase 5	41663	3.06 ± 2.78	8.01 ± 0.15	1.39	0.0369
5	K7MM57	Fungal lipase-like domain-containing protein	55970	10.97 ± 0.25	11.97 ± 0.23	0.13	0.0069
6	P29530	P24 oleosin isoform A (P89)	23502	11.51 ± 0.12	12.45 ± 0.19	0.11	0.0020
7	I1M240	Lipoxygenase (EC 1.13.11.-)	103775	10.12 ± 0.06	10.42 ± 0.07	0.04	0.0056
8	K7MYT8	SGNH hydrolase-type esterase domain-containing protein	22526	13.5 ± 0.03	0 ± 0	MOPS only	0.0000
9	C6T9X7	GDSL esterase/lipase	39402	6.11 ± 3.34	0 ± 0	MOPS only	0.0340
10	C6TM82	SGNH hydrolase-type esterase domain-containing protein	29116	11.22 ± 0.18	0 ± 0	MOPS only	0.0000
11	B3TDK5	Lipoxygenase (EC 1.13.11.-)	96726	12.69 ± 0.17	12.33 ± 0.1	−0.04	0.0382
12	I1KZI9	Fungal lipase-like domain-containing protein	54495	10.38 ± 0.94	6.71 ± 1.12	−0.63	0.0121
13	K7M5M3	Fungal lipase-like domain-containing protein	53623	7.88 ± 0.69	1.57 ± 2.72	−2.33	0.0176
14	A0A0R0FEC7	Fungal lipase-like domain-containing protein	54365	6.01 ± 0.62	1.04 ± 1.79	−2.54	0.0105
15	A0A0R0KJN8	Fungal lipase-like domain-containing protein	56402	8.49 ± 0.55	0.99 ± 1.71	−3.11	0.0019
16	I1L0D2	Patatin (EC 3.1.1.-)	46744	11.01 ± 4.61	0.5 ± 0.86	−4.47	0.0179

four proteins increased in abundance, while six decreased in the pH 7.5 MOPS/PSMA group. The proteins that increased in quantity were GDSL esterase/lipase 5 (I1KHH3), fungal lipase-like domain-containing protein (K7MM57), P24 oleosin isoform A (P29530), and lipoxygenase (I1M240). The proteins that decreased included lipoxygenase (B3TDK5), fungal lipase-like domain-containing proteins (I1KZI9, K7M5M3, A0A0R0FEC7, and A0A0R0KJN8), and patatin (I1L0D2). These altered proteins were primarily involved in lipid metabolic processes and catalytic functions (Figure 4c). Enriched molecular functions included lipase, hydrolase, and triglyceride lipase activities (Figure 4d). The altered proteins were predominantly localized in the extracellular region, lipid droplets, and extracellular space (Figure 4e). One of the major challenges in enzyme immobilization lies in achieving a balanced interaction between the enzyme and the polymer matrix. Interactions that are excessively strong can alter the native enzyme structure, whereas overly weak interactions may lead to enzyme leaching and denaturation upon direct exposure to the surrounding medium. Such imbalances may account for the reduced abundance observed for some of the aforementioned proteins. Conversely, when a balanced enzyme-polymer interaction is achieved, the immobilized enzyme is effectively shielded and stabilized by a host matrix while maintaining its active catalytic accessibility and conformational dynamics. This possibly explains the increased abundance of proteins that benefited from the PSMA-mediated extraction. The enrichment with soybean esterases and lipases (I1M1M1, I1KGH4, I1KHH3, and K7MM57) could be related to the enhanced specific lipase activity in the pH 7.5 MOPS/PSMA extracts, as compared to the MOPS-only treatment in Figure 2. Furthermore, the sample treated with pH 7.5 MOPS/PSMA buffer also yielded a higher abundance of oleosins (I1N747 and P29530), highlighting its effectiveness in recovering membrane-associated proteins. Oleosins possess a unique structural architecture with a long central hydrophobic hairpin attached to two hydrophilic arms, imparting them with an amphipathic nature for potential biosurfactants in oil−water emulsions. However, their amphiphilicity also poses significant challenges for extraction, as it restricts the selection of compatible solvents. The use of PSMA as a membrane lysis agent presents a promising strategy to effectively recover oleosin proteins without the need of exogeneous phospholipids. This phenomenon is demonstrated here for the first time.

The formation of enzyme-immobilized particles in the pH 7.5 MOPS/PSMA extracts was confirmed by both scanning electron microscopy (SEM) and dynamic light scattering (DLS). SEM images in Figure 5a and Figure 5b reveal that the MOPS/PSMA extracts contained highly uniform, round-shaped particles with smooth surfaces. According to the DLS particle size distribution plot in Figure 6a, the mean particle size diameter was around 227 ± 3 nm (PDI ∼ 0.195). The absence of visible particle aggregates in the SEM images in Figure 5b implied particle robustness, even in the dried state. In contrast, the pH 7.5 MOPS extracts did not exhibit spherical particle formation. Instead, SEM images in Figure 5c and Figure 5d showed irregular-shaped structures with open ends and rough outer surfaces (arrows). Based on SEM measurements in Figure 5c, the smallest unit of these structures showed an average diameter of around 2−3 μm. This contributes to a broad tail region (700−900 nm) in the DLS plot in Figure 6a. We noted that the DLS-derived diameter appears slightly smaller than the apparent sizes observed in SEM. DLS measures the hydrodynamic diameter of dispersed particles in solution, reflecting their diffusion behavior in the solvated state, whereas SEM provides the projected dimension of dried particles under vacuum. The drying process and loss of the hydration shell often cause particle coalescence, resulting in larger sizes in SEM micrographs. Such artifactual aggregation has been well-documented as a potential limitation of electron microscopic techniques.[57−59]

https://doi.org/10.1021/acsomega.5c09274
ACS Omega 2026, 11, 5608−5621

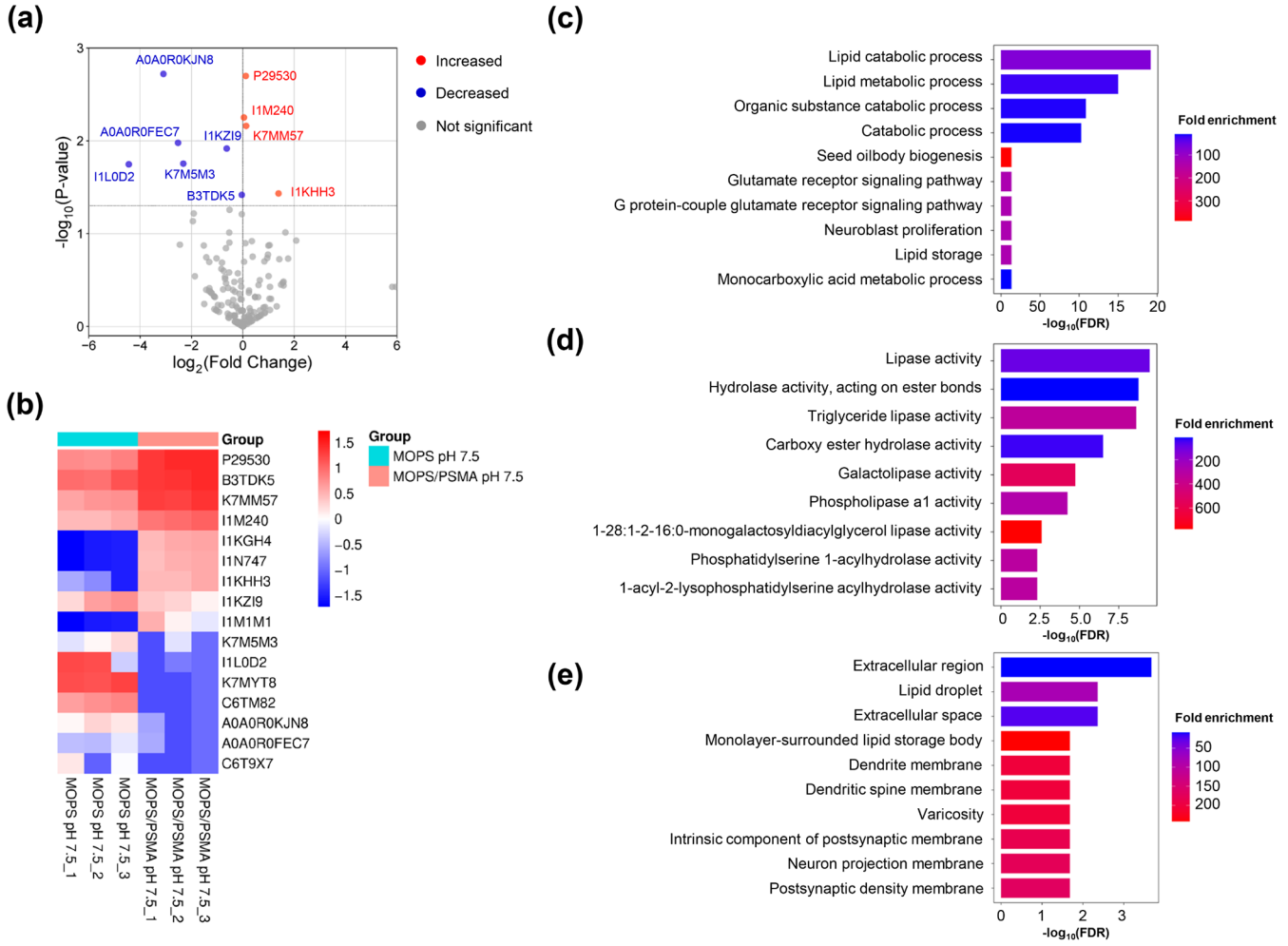

Figure 4. Comparative analysis of protein profiles of crude soybean extracts treated with pH 7.5 MOPS buffer and pH 7.5 MOPS/PSMA buffer. (a) Volcano plot displaying differentially expressed proteins. (b) Heatmap representing significantly altered proteins between the two sample groups. (c–e) Bar plots of the most enriched GO terms categorized by (c) biological process, (d) molecular function, and (e) cellular component.

A comparison of the specific lipase activity between commercial wheat germ lipase and soybean extracts yielded interesting findings. As illustrated in Figure 6b, the commercial enzyme exhibited a specific lipase activity around 1.5 mU/mg, whereas those obtained by the pH 7.5 MOPS extraction (free-enzymes) and pH 7.5 MOPS/PSMA extraction (immobilized enzymes) displayed a significantly higher enzymatic activity around 5.7 mU/mg. This finding suggested that the soybean extracts have a stronger affinity toward the pNPB substrate, likely due to the synergistic effects of different proteins listed in Table 1. In an effort to prepare electrospun catalytic membranes, soybean extracts were mixed with an aqueous PVA solution prior to the electrospinning process. The successful incorporation of enzyme-loaded electrospun PVA membranes was confirmed by the FT-IR spectrum, which displayed characteristic protein bands at 1,637 cm^{-1} and 1,545 cm^{-1}, corresponding to the amide I (C═O stretching) and amide II (N−H bending and C−N stretching) vibrations, respectively. These bands coexist with the typical absorption peaks of PVA, including the broad O−H stretching band at 3,316 cm^{-1} and the C−O stretching at 1,089 cm^{-1}. Additionally, a band at 1,732 cm^{-1} attributed to the C═O stretching of residual acetyl groups indicated partial hydrolysis of the PVA backbone (see Supplementary Figure S3). To verify that neither PVA matrix nor the electrospinning process adversely affected the catalytic profile of soybean extracts, the specific lipase activities for both pre-spun solutions and their electrospun fibers were examined. A series of PVA solutions containing different weight proportions of soybean extracts (1%, 2%, and 4% w/v) was prepared and analyzed using the pNPB assay. All solutions in Figure 7 exhibited a reduced specific lipase activity when compared to the PVA-free enzyme formulations in Figure 6b. This substantial loss of enzyme activity is attributed to an enzyme-PVA binding effect, which may hinder the formation of the enzyme−substrate complex and thereafter restrict catalytic efficiency. A strong polar interaction between soybean enzymes and PVA molecules was further supported by a significant increase in the viscosity of the solutions in Figure 8a, especially at 4% enzyme loading. This scenario was offset when they were processed into electrospun fibers. As shown in Figure 7, most of the redissolved nanofibers containing free-enzymes and immobilized enzymes exhibited a remarkably higher specific lipase activity, as compared to their corresponding solutions. For example, the solution with 1% immobilized enzymes showed a specific lipase activity of around 1.6 mU/mg, whereas the corresponding nanofibers displayed a value of 5.9 mU/mg, nearly identical to that of the native immobilized enzymes in

https://doi.org/10.1021/acsomega.5c09274
ACS Omega 2026, 11, 5608−5621

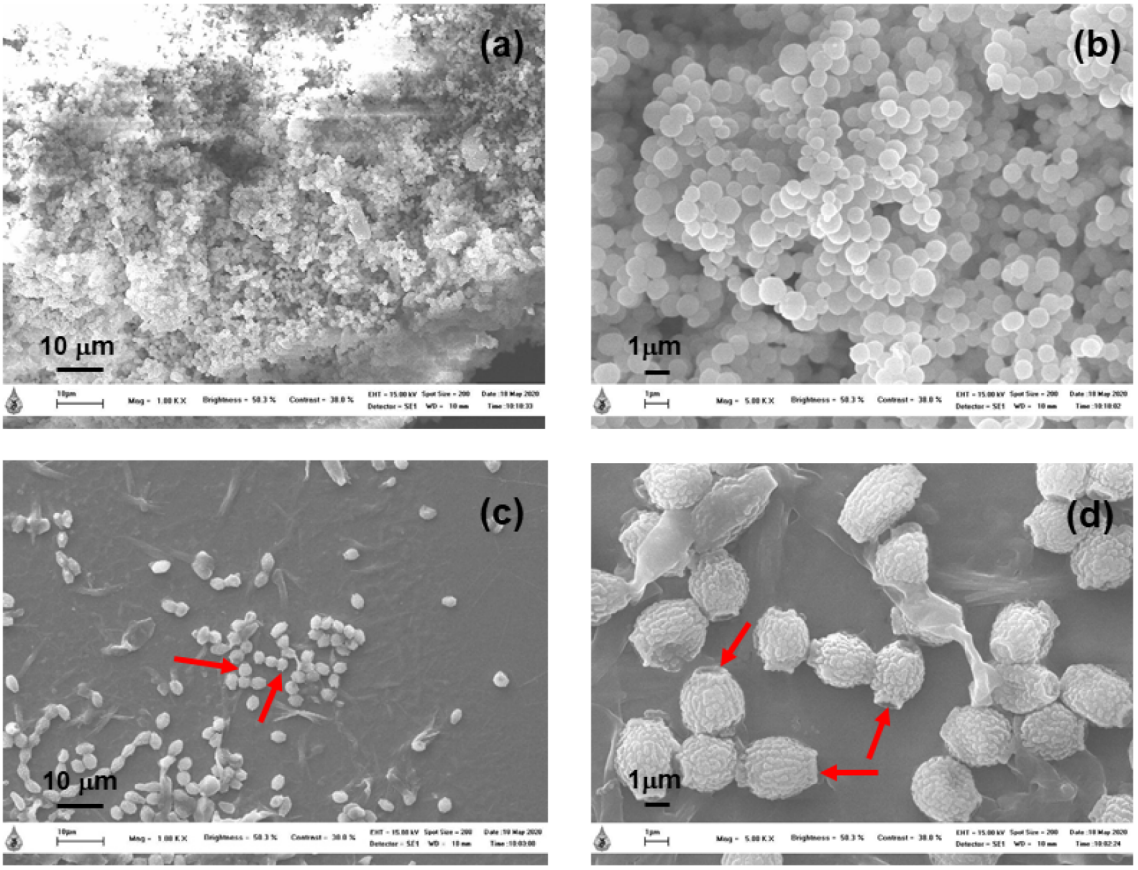

Figure 5. SEM images of soybean crude extracts using either: (a, b) pH 7.5 MOPS/PSMA buffer, or (c, d) pH 7.5 MOPS buffer. All extractions were conducted at 25 °C for 45 min with a mass-to-buffer volume ratio (m/v) of 1:25. SEM micrographs in panels (a) and (c) were acquired at a magnification of 1.0 kX, while those in panels (b) and (d) were taken at 5.0 kX.

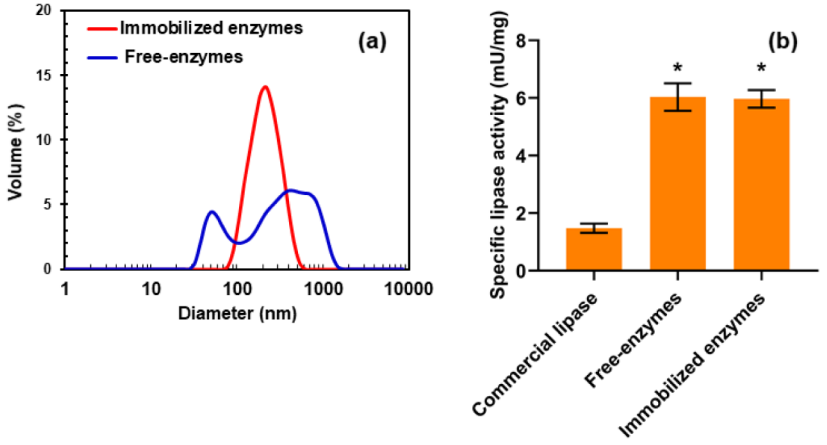

Figure 6. (a) DLS size distribution profiles of free-enzyme molecules and immobilized enzyme particles. The extraction was performed at 25 °C for 45 min using an m/v ratio of 1:25. (b) Comparison of the specific lipase activities among different enzyme solutions (1% w/v). Data are expressed as mean ± SD (n = 3). Asterisks (*) indicate significant differences compared to the commercial lipase (P < 0.01).

Figure 6b. A similar trend was also reported in the case of commercial enzyme sources.[12,60] This suggested that the enzyme activity was mostly retained, and the undesirable binding effect with PVA could be minimized. A possible explanation is that electrospinning induces chain orientation within the PVA matrix.[61] Upon dissolution, the oriented PVA chains may retain a closer spatial arrangement compared to their configuration in the solution, thereby decreasing the accessibility for enzymatic interaction. Additionally, as demonstrated in Figure 7, the nanofibers with immobilized enzymes generally displayed a higher specific lipase activity than those with the free-enzymes. To further elucidate this phenomenon, additional DLS measurements were performed on the redissolved PVA electrospun membranes (1% w/v in deionized water), and the comparative results are presented in Supplementary Figure S4. The neat PVA membranes primarily showed a monomodal distribution profile centered at approximately at 16 nm, corresponding to single-chain PVA

https://doi.org/10.1021/acsomega.5c09274
ACS Omega 2026, 11, 5608−5621

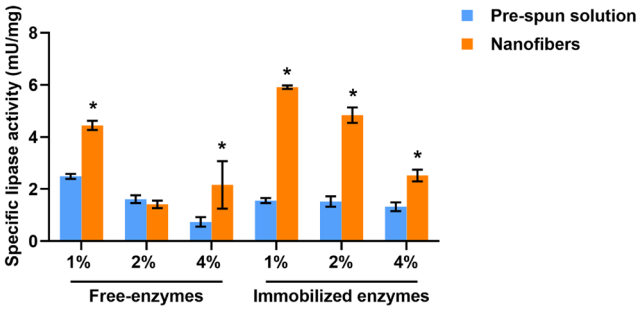

Figure 7. Effect of enzyme loading concentration (1%, 2%, and 4% w/v) on the specific lipase activities of the pre-spun solutions (blue bars) and their corresponding electrospun nanofibers (orange bars). The soybean enzymes are in the form of free-enzymes and immobilized enzymes. Data are expressed as mean ± SD (n = 3). Asterisks (*) indicate significant differences compared to the pre-spun solution (P < 0.01).

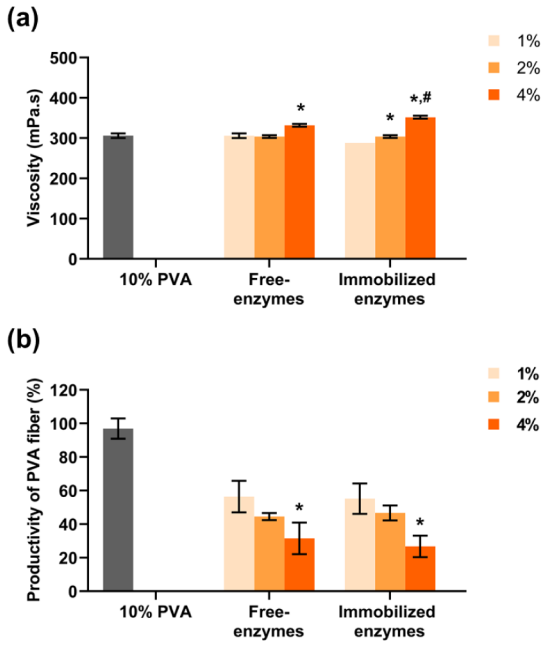

Figure 8. Effects of enzyme loading on: (a) viscosity of pre-spun solutions, and (b) productivity of PVA fibers. Two different enzyme types are free-enzymes and immobilized enzymes. Data are expressed as mean ± SD (n = 3). Asterisks (*) and number sign (#) denote values statistically significant relative to the 1% and 2% enzyme loading levels, respectively (P < 0.001). Viscosity and fiber mass productivity of the 10% (w/v) PVA solution were also presented for comparison in (a) and (b), respectively.

coils in aqueous solution.[62,63] The free-enzymes showed a bimodal distribution profile with an additional micron-sized population (1−2 μm), suggesting the possibility of enzyme-PVA microgel coassembly and partial enzyme aggregation during electrospinning, which may account for its lower catalytic activity. The immobilized-enzyme membranes, however, exhibited a dominant population around 10−20 nm and a weak secondary hump (600−700 nm), likely corresponding to the PVA coils and coassembled PSMA-enzyme-PVA microgels, respectively. The hydrated microgel environment and PSMA shielding effect likely help maintain the enzyme's conformation and functionality,[64−66] consistent with the higher apparent enzymatic activity observed for the immobilized-enzyme membranes (Figure 7). It should be noted that the enzyme activity measurements in Figure 7 were performed after dissolving the electrospun PVA membrane in aqueous media. These data thus confirm that the immobilized enzymes remain active after electrospinning but do not directly represent the solid-state catalysis in the intact membranes. Nonetheless, previous studies have demonstrated that lipases confined within PVA-based electrospun membranes can retain catalytic activity, stability, and reusability under solid-state or biphasic reaction conditions, supporting the potential functionality of the intact membranes even without dissolution.[67,68]

To examine the effect of enzyme loading on electrospinnability of PVA fibers, the mass yield rates (g/h) of the PVA membranes were examined both in the presence and in the absence of soybean enzymes. The results are expressed as a percentage of productivity of PVA fibers (%) based on the yield of the PVA-only membrane (0.136 ± 0.008 g/h). As demonstrated in Figure 8b, the productivity of electrospun PVA fibers decreased with enzyme loading concentration. At 1% loading, the productivity of PVA fibers decreased to around 57−58% for both free-enzymes and immobilized enzymes. The incremental increase in enzyme loading up to 4% significantly reduced fiber productivity to around 28−32%. Results demonstrate a negative impact of enzyme incorporation on the productivity of the electrospun PVA fibrous membranes. Despite this, the enzyme-immobilized PVA membrane (1% loading) retained catalytic activity (Figure 7), demonstrating its strong potential as a biocatalytic substrate beyond that of conventional PVA membranes.

In addition to evaluating productivity, we also examined the impact of enzyme incorporation on fiber morphology by using scanning electron microscopy (SEM). As shown in Figure 9, the neat PVA membrane (0% enzyme loading) exhibited uniform and smooth nanofibers with a mean diameter of approximately 138 ± 31 nm. Upon enzyme addition, a gradual increase in fiber diameter was observed, reaching 275 ± 117 nm for the immobilized enzyme system and 249 ± 164 nm for the free-enzyme system. Although the diameter change at low enzyme content was not statistically significant (Supplementary Figure S5), high-magnification SEM images in Figure 9 revealed localized regions of fiber merging (highlighted by red circles and ovals). This phenomenon became progressively more pronounced with high enzyme concentrations, particularly at 4% (w/v), wherein extensive fiber coalescence was clearly observed. Moreover, the 4% free-enzyme-loaded fibers exhibited elongated bead structures (indicated by red arrows). These findings collectively suggest the existence of a critical enzyme-loading threshold beyond which the morphological integrity of the PVA electrospun fibers is adversely affected. The reduced fiber-forming ability may be due to the change in solution viscosity, as shown in Figure 8a. Increased solution viscosity via enzyme addition enhances the flow resistance and restricts axial elongation during electrospinning. This can lead to the production of thicker fibers or merging of fibers, as depicted in Figure 9. Moreover, differences in hydrophilicity and solubility parameters between proteins and polymers, particularly in organic solvent systems, can induce microphase separation, thereby disrupting jet homogeneity and resulting in discontinuous fiber formation.[69] The distinct protein−solvent and polymer−solvent interactions may also modify solvent evaporation kinetics.[20] Slower or uneven evaporation can cause fiber collapse or fusion on the collector, diminishing overall

https://doi.org/10.1021/acsomega.5c09274
ACS Omega 2026, 11, 5608−5621

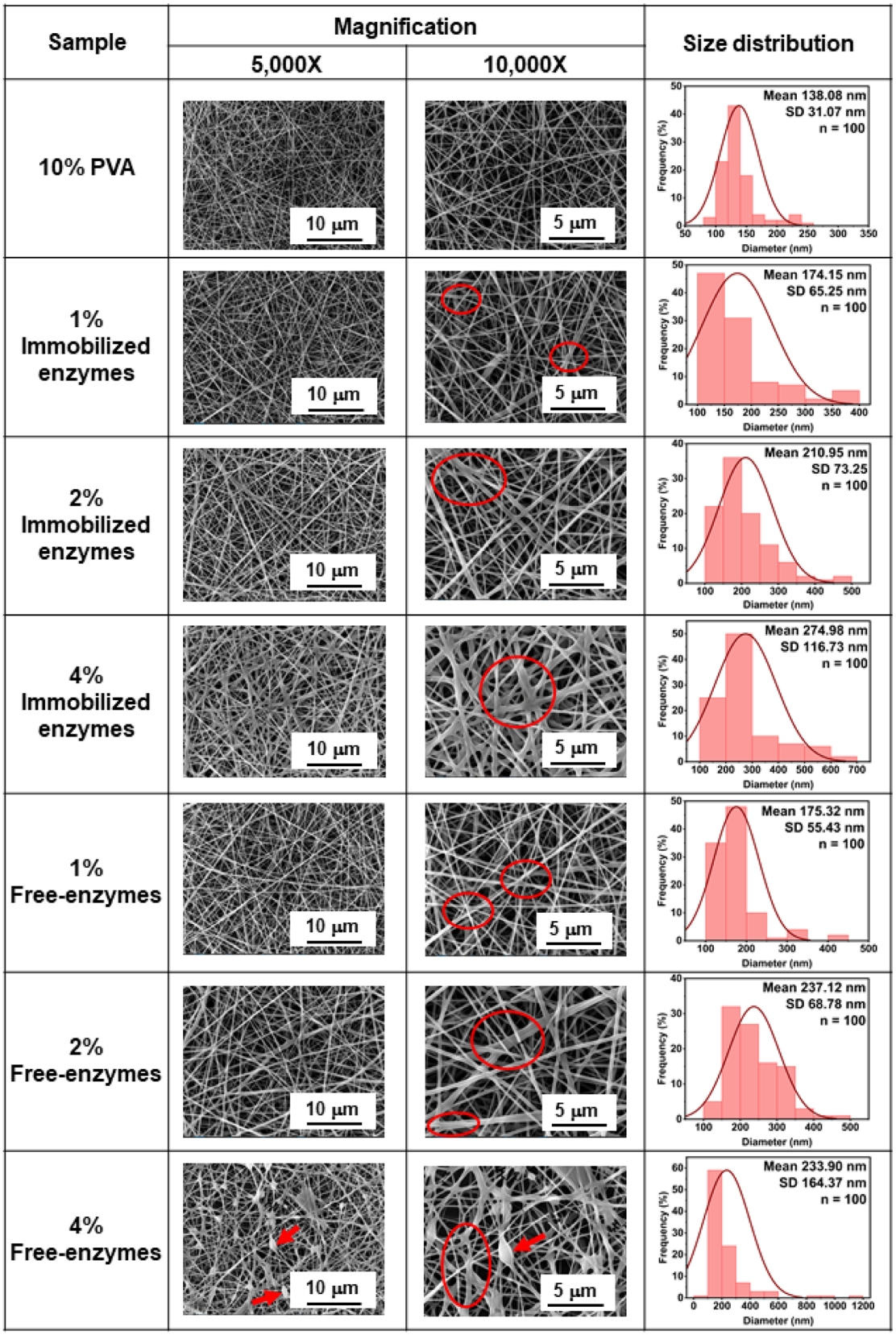

Figure 9. Effect of enzyme loading concentration on fibemorphology and size distribution of electrospun fibers prepared from 10% aqueous PVA solutions. Two different enzyme types are immobilized enzymes and free-enzymes.

fiber uniformity and productivity. Nevertheless, partial fusion or welding at fiber junctions may provide mechanical benefits by increasing the tensile modulus of the electrospun membrane, thus enhancing its reusability and suitability for practical applications. To ensure uniform fiber morphology and maintain acceptable production yields, a maximum

https://doi.org/10.1021/acsomega.5c09274
ACS Omega 2026, 11, 5608−5621

enzyme loading of 1% (w/v) was recommended. Despite the deleterious impact of soybean enzymes on PVA electrospinnability, this study successfully demonstrates the fabrication of ultrafine fibrous membranes embedded with lipolytic enzymes for potential use in biocatalytic processes, biosensors, and tissue engineering scaffolds.

4. CONCLUSION

The present study demonstrated the dual capability of poly(styrene-*alt*-maleic acid) (PSMA) as both a membrane-lysis and enzyme-immobilization agent, enabling the direct extraction of soybean lipolytic enzymes into nanometeric PSMA-protein complexes. Systematic evaluation of extraction parameters identified pH 7.5 and a soybean mass-to-buffer volume ratio of 1:25 as optimal processing conditions, yielding a maximum specific lipase activity of 16 mU/mg. Comparative proteomic profiling revealed 16 differentially expressed proteins associated with lipid metabolism in MOPS/PSMA-treated soybean extracts, confirming selective enrichment of lipolytic enzymes. The resulting enzyme-PSMA nanoparticles exhibited a homogeneous morphology with a mean diameter of ∼227 nm and were successfully incorporated (1% w/v) into electrospun poly(vinyl alcohol) (PVA) membranes, producing uniform nanofibers (174 ± 65 nm) without bead formation. At this loading, the immobilized enzymes retained nearly full activity toward *p*-nitrophenyl butyrate (pNPB), demonstrating minimal deactivation during electrospinning. Remarkably, the particle-loaded PVA fibrous membrane exhibited a nearly 3-fold increase in specific lipase activity as compared with that loaded with the free-enzyme molecules, implying that the synergistic effects of PSMA self-assembly and hydrating PVA microgels effectively prevented protein denaturation and enhanced catalytic accessibility. This integrated PSMA-assisted extraction and electrospinning strategy offers an efficient and scalable route for enzyme recovery, stabilization, and immobilization, providing a versatile platform for high-performance biocatalytic membranes applicable to the pharmaceutical, biofuel, and food processing industries.

5. HIGHLIGHTS

- A one-step method was developed for simultaneous extraction and immobilization of soybean lipolytic enzymes.
- Optimized at pH 7.5 and a 1:25 mass-to-buffer ratio, the process achieved a maximum specific lipase activity of 16 mU/mg.
- Proteomic profiling identified 16 proteins linked to lipid metabolism and lipase function.
- Electrospinning of PVA with 1% (w/v) enzyme-loaded particles produced 174 nm nanofibers.
- These fibers showed a threefold increase in enzyme activity, demonstrating strong potential for efficient biocatalytic applications.

■ ASSOCIATED CONTENT

Data Availability Statement

The data that support the findings of this study are available on request from the corresponding author. The raw MS/MS spectral data are available on the ProteomeXchange repository under registration numbers JPST004124 (https://repository.jpostdb.org/preview/204500789868f2cacdbc4db; Access key: 2255) and PXD069519.

Supporting Information

The Supporting Information is available free of charge at https://pubs.acs.org/doi/10.1021/acsomega.5c09274.

Additional figures (Figures S1−S5) and a table (Table S1) (PDF)

■ AUTHOR INFORMATION

Corresponding Author

Patchara Punyamoonwongsa − *School of Science, Mae Fah Luang University, Chiang Rai 57100, Thailand;* orcid.org/0000-0003-2058-6320; Email: patchara@mfu.ac.th

Authors

Kamonchanok Thananukul − *School of Science, Mae Fah Luang University, Chiang Rai 57100, Thailand*

Patnarin Worajittiphon − *Department of Chemistry, Faculty of Science, Chiang Mai University, Chiang Mai 50200, Thailand;* orcid.org/0000-0002-7498-8416

Kitiphong Khongphinitbunjong − *School of Science, Mae Fah Luang University, Chiang Rai 57100, Thailand*

Orawan Suwantong − *School of Science, Mae Fah Luang University, Chiang Rai 57100, Thailand; Center of Chemical Innovation for Sustainability (CIS), Mae Fah Luang University, Chiang Rai 57100, Thailand*

Sittiruk Roytrakul − *National Center for Genetic Engineering and Biotechnology, Pathum Thani 12120, Thailand*

Siripat Aluksanasuwan − *School of Medicine, Mae Fah Luang University, Chiang Rai 57100, Thailand; Cancer and Immunology Research Center (CIRC), Mae Fah Luang University, Chiang Rai 57100, Thailand;* orcid.org/0000-0002-3542-5880

Matthew J. Derry − *Aston Institute for Membrane Excellence, Aston University, Birmingham B4 7ET, United Kingdom;* orcid.org/0000-0001-5010-6725

Paul D. Topham − *Aston Institute for Membrane Excellence, Aston University, Birmingham B4 7ET, United Kingdom;* orcid.org/0000-0003-4152-6976

Complete contact information is available at: https://pubs.acs.org/10.1021/acsomega.5c09274

Author Contributions

K.T.: Methodology, Investigation, Formal analysis, and Writing—original draft. K.K., O.S., and P.W.: Writing—review and editing. S.R.: Methodology, Investigation, and Validation. S.A.: Formal analysis and Writing—review and editing. M.J.D. and P.D.T.: Writing—data analysis, Manuscript review and editing. P.P.: Writing—review and editing, Writing—original draft, Validation, Methodology, Funding acquisition, Formal analysis, and Conceptualization.

Notes

The authors declare no competing financial interest.

■ ACKNOWLEDGMENTS

This work was supported by Mae Fah Luang University, Thailand Science Research and Innovation (TSRI), as well as the National Science, Research and Innovation Fund (NSRF) [grant no. 662A01009]. This research received financial support from Mae Fah Luang University under a Postdoctoral Fellowship Program [grant no.01/2567]. The research activities were partly supported by the European Union's

https://doi.org/10.1021/acsomega.5c09274
ACS Omega 2026, 11, 5608−5621

Horizon 2020 Research and Innovation Program under the Marie Skłodowska-Curie grant agreement no. 871650 (MED-IPOL), as well as the Hub of Talents in Bioplastics for Use in Medical Applications, National Research Council of Thailand (NRCT) [grant No. N34E670071]. The Aston Institute for Membrane Excellence (AIME) is funded by UKRI's Research England as part of their Expanding Excellence in England (E3) fund. The project was also supported by Reinventing University 2026, which has received funding from the Office of the Permanent Secretary of the Ministry of Higher Education, Science, Research and Innovation, Thailand.

REFERENCES

(1) Sajeev, S. C.; Deshmukh, R., *Enzymes Market*; Allied Market Research, 2025; https://www.alliedmarketresearch.com/enzymes-market, 2022.
(2) Angelo, A. J.; Ory, R. L. Lipid degradation during seed deterioration. *Phytopathology*. **1983** *73* 10.1094. .
(3) Gadge, P. P.; Madhikar, S. D.; Yewle, J. N.; Jadhav, U. U.; Chougale, A. D.; Zambare, V. P.; Padul, M. V. Biochemical studies of lipase from germinating oil seeds (*Glycine max*). *Am. J. Biochem. Biotechnol.* **2011**, *7* (3), 141−145.
(4) de Barros, M.; Macedo, G. A. Biochemical characterization of esterase from soybean (*Glycine max L.*). *Food Sci. Biotechnol.* **2011**, *20* (5), 1195−1201.
(5) Huang, X.-J.; Yu, A.-G.; Xu, Z.-K. Covalent immobilization of lipase from Candida rugosa onto poly (acrylonitrile-*co*-2-hydroxyethyl methacrylate) electrospun fibrous membranes for potential bioreactor application. *Bioresour. Technol.* **2008**, *99* (13), 5459−5465.
(6) Wang, F.; Nie, T. T.; Shao, L. L.; Cui, Z. Comparison of physical and covalent immobilization of lipase from Candida antarctica on polyamine microspheres of alkylamine matrix. *Biocatal. Biotransform.* **2014**, *32* (5−6), 314−326.
(7) Xing, C.; Mei, P.; Mu, Z.; Li, B.; Feng, X.; Zhang, Y.; Wang, B. Enhancing enzyme activity by the modulation of covalent interactions in the confined channels of covalent organic frameworks. *Angew. Chem.* **2022**, *134* (21), No. e202201378.
(8) Oktay, B.; Demir, S.; Kayaman-Apohan, N. Immobilization of α-amylase onto poly (glycidyl methacrylate) grafted electrospun fibers by ATRP. *Mater. Sci. Eng.: C* **2015**, *50*, 386−393.
(9) Medina-Castillo, A. L.; Ruzic, L.; Nidetzky, B.; Bolivar, J. M. Hydrophilic nonwoven nanofiber membranes as nanostructured supports for enzyme immobilization. *ACS Appl. Polym. Mater.* **2022**, *4* (8), 6054−6066.
(10) Makas, Y. G.; Kalkan, N. A.; Aksoy, S.; Altinok, H.; Hasirci, N. Immobilization of laccase in κ-carrageenan based semi-interpenetrating polymer networks. *J. Biotechnol.* **2010**, *148* (4), 216−220.
(11) Horn, C.; Pospiech, D.; Allertz, P. J.; Müller, M.; Salchert, K.; Hommel, R. Chemical design of hydrogels with immobilized laccase for the reduction of persistent trace compounds in wastewater. *ACS Appl. Polym. Mater.* **2021**, *3* (5), 2823−2834.
(12) Sóti, P. L.; Weiser, D.; Vigh, T.; Nagy, Z. K.; Poppe, L.; Marosi, G. Electrospun polylactic acid and polyvinyl alcohol fibers as efficient and stable nanomaterials for immobilization of lipases. *Bioprocess Biosyst. Eng.* **2016**, *39* (3), 449−459.
(13) Sakai, S.; Antoku, K.; Yamaguchi, T.; Kawakami, K. Development of electrospun poly (vinyl alcohol) fibers immobilizing lipase highly activated by alkyl-silicate for flow-through reactors. *J. Membr. Sci.* **2008**, *325* (1), 454−459.
(14) Kaur, H.; Singh, S.; Rode, S.; Chaudhary, P. K.; Khan, N. A.; Ramamurthy, P. C.; Gupta, D. N.; Kumar, R.; Das, J.; Sharma, A. K. Fabrication and characterization of polyvinyl alcohol-chitosan composite nanofibers for carboxylesterase immobilization to enhance the stability of the enzyme. *Sci. Rep.* **2024**, *14* (1), 19615.
(15) Fard, G. C.; Gashti, M. P.; Dehdast, S. A.; Shabani, M.; Zarinabadi, E.; Seifi, N.; Berenjian, A. Novel polyamide/chitosan nanofibers containing glucose oxidase and rosemary extract: fabrication and antimicrobial functionality. *Coatings* **2024**, *14* (4), 411.
(16) Balcioğlu, S. Immobilization of α-amylase on electrospun polycaprolactone (PCL)/chitosan (CHI) nanofibers: a novel approach to improve enzyme stability and performance. *Int. J. Polym. Anal. Charact.* **2025**, 1−16.
(17) Amani, A.; Kalajahi, S. T.; Yazdian, F.; Mirzababaei, S.; Rashedi, H.; Faramarzi, M. A.; Vahidi, M. Immobilization of urease enzyme on chitosan/polyvinyl alcohol electrospun nanofibers. *Biotechnol. Prog.* **2022**, *38* (5), No. e3282.
(18) Işik, C.; Teke, M. Fabrication of electrospun cellulose-derived nanofiber membranes with enhanced stability properties of arginase. *Turk. J. Chem.* **2022**, *46* (4), 1164−1175.
(19) Adlercreutz, P. Immobilisation and application of lipases in organic media. *Chem. Soc. Rev.* **2013**, *42* (15), 6406−6436.
(20) Nikmaram, N.; Roohinejad, S.; Hashemi, S.; Koubaa, M.; Barba, F. J.; Abbaspourrad, A.; Greiner, R. Emulsion-based systems for fabrication of electrospun nanofibers: Food, pharmaceutical and biomedical applications. *RSC Adv.* **2017**, *7* (46), 28951−28964.
(21) Tóth, G. D.; Kazsoki, A.; Gyarmati, B.; Szilágyi, A.; Vasvári, G.; Katona, G.; Szente, L.; Zelkó, R.; Poppe, L.; Balogh-Weiser, D.; et al. Nanofibrous formulation of cyclodextrin stabilized lipases for efficient pancreatin replacement therapies. *Pharmaceutics* **2021**, *13* (7), 972.
(22) Li, J.; Wang, H.; Wang, L.; Yu, D.; Zhang, X. Stabilization effects of saccharides in protein formulations: A review of sucrose, trehalose, cyclodextrins and dextrans. *Eur. J. Pharm. Sci.* **2024**, *192*, 106625.
(23) Moreira, A.; Lawson, D.; Onyekuru, L.; Dziemidowicz, K.; Angkawinitwong, U.; Costa, P. F.; Radacsi, N.; Williams, G. R. Protein encapsulation by electrospinning and electrospraying. *J. Controlled Release* **2021**, *329*, 1172−1197.
(24) Chandrawati, R.; Olesen, M. T. J.; Marini, T. C. C.; Bisra, G.; Guex, A. G.; de Oliveira, M. G.; Zelikin, A. N.; Stevens, M. M. Enzyme prodrug therapy engineered into electrospun fibers with embedded liposomes for controlled, localized synthesis of therapeutics. *Adv. Healthcare Mater.* **2017**, *6* (17), 1700385.
(25) Karakas, C. Y.; Ustundag, C. B.; Sahin, A.; Karadag, A. Co-axial electrospinning of liposomal propolis loaded gelatin-zein fibers as a potential wound healing material. *J. Appl. Polym. Sci.* **2023**, *140* (46), No. e54683.
(26) Asadi, V.; Marandi, A.; Kardanpour, R.; Tangestaninejad, S.; Moghadam, M.; Mirkhani, V.; Mohammadpoor-Baltork, I.; Mirzaei, R. Carbonic anhydrase-embedded ZIF-8 electrospun PVA fibers as an excellent biocatalyst candidate. *ACS Omega* **2023**, *8* (20), 17809−17818.
(27) Buachi, C.; Thananukul, K.; Khongphinitbunjong, K.; Molloy, R.; Punyamoonwongsa, P. A single-step extraction and immobilization of soybean lipolytic enzymes by using a purpose-designed copolymer of styrene and maleic acid as a membrane lysis agent. *Heliyon* **2024**, *10* (10), No. e31313.
(28) Xue, M.; Cheng, L.; Faustino, I.; Guo, W.; Marrink, S. J. Molecular mechanism of lipid nanodisk formation by styrene-maleic acid copolymers. *Biophys. J.* **2018**, *115* (3), 494−502.
(29) Iyer, A. K.; Greish, K.; Fang, J.; Murakami, R.; Maeda, H. High-loading nanosized micelles of copoly(styrene−maleic acid)−zinc protoporphyrin for targeted delivery of a potent heme oxygenase inhibitor. *Biomaterials* **2007**, *28* (10), 1871−1881.
(30) Parayath, N. N.; Nehoff, H.; Norton, S. E.; Highton, A. J.; Taurin, S.; Kemp, R. A.; Greish, K. Styrene maleic acid-encapsulated paclitaxel micelles: antitumor activity and toxicity studies following oral administration in a murine orthotopic colon cancer model. *Int. J. Nanomed.* **2016**, *11*, 3979−3991.
(31) Greish, K.; Taha, S.; Jasim, A.; Elghany, S. A.; Sultan, A.; AlKhateeb, A.; Othman, M.; Jun, F.; Taurin, S.; Bakhiet, M. Styrene maleic acid encapsulated raloxifene micelles for management of inflammatory bowel disease. *Clin. Transl. Med.* **2017**, *6*, 1.
(32) Martey, O.; Nimick, M.; Taurin, S.; Sundararajan, V.; Greish, K.; Rosengren, R. J. Styrene maleic acid-encapsulated RL71 micelles

https://doi.org/10.1021/acsomega.5c09274
ACS Omega 2026, 11, 5608−5621

suppress tumor growth in a murine xenograft model of triple negative breast cancer. *Int. J. Nanomed.* **2017**, *12*, 7225−7237.
(33) Sütekin, S. D.; Atıcı, A. B.; Güven, O.; Hoffman, A. S. Controlling of free radical copolymerization of styrene and maleic anhydride via RAFT process for the preparation of acetaminophen drug conjugates. *Radiat. Phys. Chem.* **2018**, *148*, 5−12.
(34) Morrison, K. A.; Akram, A.; Mathews, A.; Khan, Z. A.; Patel, J. H.; Zhou, C.; Hardy, D. J.; Moore-Kelly, C.; Patel, R.; Odiba, V.; et al. Membrane protein extraction and purification using styrene−maleic acid (SMA) copolymer: effect of variations in polymer structure. *Biochem. J.* **2016**, *473* (23), 4349−4360.
(35) Liu, Y.; Moura, E. C. C. M.; Dörr, J. M.; Scheidelaar, S.; Heger, M.; Egmond, M. R.; Killian, J. A.; Mohammadi, T.; Breukink, E. Bacillus subtilis MraY in detergent-free system of nanodiscs wrapped by styrene-maleic acid copolymers. *PLoS One* **2018**, *13* (11), No. e0206692.
(36) Korotych, O.; Mondal, J.; Gattás-Asfura, K. M.; Hendricks, J.; Bruce, B. D. Evaluation of commercially available styrene-co-maleic acid polymers for the extraction of membrane proteins from spinach chloroplast thylakoids. *Eur. Polym. J.* **2019**, *114*, 485−500.
(37) Scheidelaar, S.; Koorengevel, M. C.; van Walree, C. A.; Dominguez, J. J.; Dörr, J. M.; Killian, J. A. Effect of polymer composition and pH on membrane solubilization by styrene-maleic acid copolymers. *Biophys. J.* **2016**, *111* (9), 1974−1986.
(38) Hall, S. C. L.; Tognoloni, C.; Price, G. J.; Klumperman, B.; Edler, K. J.; Dafforn, T. R.; Arnold, T. Influence of poly (styrene-co-maleic acid) copolymer structure on the properties and self-assembly of SMALP nanodiscs. *Biomacromolecules* **2018**, *19* (3), 761−772.
(39) Shinde, P.; Musameh, M.; Gao, Y.; Robinson, A. J.; Kyratzis, I. L. Immobilization and stabilization of alcohol dehydrogenase on polyvinyl alcohol fibre. *Biotechnol. Rep.* **2018**, *19*, No. e00260.
(40) Guajardo, N. Immobilization of lipases using poly (vinyl) alcohol. *Polymers* **2023**, *15* (9), 2021.
(41) Zahra, F. T.; Quick, Q.; Mu, R. Electrospun PVA fibers for drug delivery: A review. *Polymers* **2023**, *15* (18), 3837.
(42) Park, J.-C.; Ito, T.; Kim, K.-O.; Kim, K.-W.; Kim, B.-S.; Khil, M.-S.; Kim, H.-Y.; Kim, I.-S. Electrospun poly (vinyl alcohol) nanofibers: effects of degree of hydrolysis and enhanced water stability. *Polym. J.* **2010**, *42* (3), 273−276.
(43) Lee, D.-W.; Koh, Y.-S.; Kim, K.-J.; Kim, B.-C.; Choi, H.-J.; Kim, D.-S.; Suhartono, M. T.; Pyun, Y.-R. Isolation and characterization of a thermophilic lipase from Bacillus thermoleovorans ID-1. *FEMS Microbiol. Lett.* **1999**, *179* (2), 393−400.
(44) Peterson, G. L. A simplification of the protein assay method of Lowry et al. which is more generally applicable. *Anal. Biochem.* **1977**, *83* (2), 346−356.
(45) Laemmli, U. K. Cleavage of structural proteins during the assembly of the head of bacteriophage T4. *Nature* **1970**, *227* (5259), 680−685.
(46) Blum, H.; Beier, H.; Gross, H. J. Improved silver staining of plant proteins, RNA and DNA in polyacrylamide gels. *Electrophoresis* **1987**, *8* (2), 93−99.
(47) Tyanova, S.; Temu, T.; Cox, J. The MaxQuant computational platform for mass spectrometry-based shotgun proteomics. *Nat. Protoc.* **2016**, *11* (12), 2301−2319.
(48) Ge, S. X.; Jung, D.; Yao, R. ShinyGO: a graphical gene-set enrichment tool for animals and plants. *Bioinformatics* **2020**, *36* (8), 2628−2629.
(49) Tang, D.; Chen, M.; Huang, X.; Zhang, G.; Zeng, L.; Zhang, G.; Wu, S.; Wang, Y. SRplot: A free online platform for data visualization and graphing. *PLoS One* **2023**, *18* (11), No. e0294236.
(50) Silva, J. N.; Godoy, M. G.; Gutarra, M. L. E.; Freire, D. M. G. Impact of extraction parameters on the recovery of lipolytic activity from fermented babassu cake. *PLoS One* **2014**, *9* (8), No. e103176.
(51) Lee, D. H.; Kim, J. M.; Shin, H. Y.; Kim, S. W. Optimization of lipase pretreatment prior to lipase immobilization to prevent loss of activity. *J. Microbiol. Biotechnol.* **2007**, *17* (4), 650.
(52) Morrison, K. A.; Wood, L.; Edler, K. J.; Doutch, J.; Price, G. J.; Koumanov, F.; Whitley, P. Membrane extraction with styrene-maleic acid copolymer results in insulin receptor autophosphorylation in the absence of ligand. *Sci. Rep.* **2022**, *12* (1), 3532.
(53) Saez-Martinez, V.; Punyamoonwongsa, P.; Tighe, B. J. Polymer−lipid interactions: Biomimetic self-assembly behaviour and surface properties of poly (styrene-*alt*-maleic acid) with diacylphosphatidylcholines. *React. Funct. Polym.* **2015**, *94*, 9−16.
(54) Fang, J.; Gao, S.; Islam, R.; Nema, H.; Yanagibashi, R.; Yoneda, N.; Watanabe, N.; Yasuda, Y.; Nuita, N.; Zhou, J.-R.; et al. Styrene maleic acid copolymer-based micellar formation of temoporfin (SMA@ mTHPC) behaves as a nanoprobe for tumor-targeted photodynamic therapy with a superior safety. *Biomedicines* **2021**, *9* (10), 1493.
(55) Banshoya, K.; Kaneo, Y.; Tanaka, T.; Yamamoto, S.; Maeda, H. Development of an amphotericin B micellar formulation using cholesterol-conjugated styrene-maleic acid copolymer for enhancement of blood circulation and antifungal selectivity. *Int. J. Pharm.* **2020**, *589*, 119813.
(56) Buachi, C.; Thammachai, C.; Tighe, B. J.; Topham, P. D.; Molloy, R.; Punyamoonwongsa, P. Encapsulation of propolis extracts in aqueous formulations by using nanovesicles of lipid and poly (styrene-*alt*-maleic acid). *Artif. Cells, Nanomed., Biotechnol.* **2023**, *51* (1), 192−204.
(57) Ramangkoon, S.; Tighe, B. J.; Derry, M. J.; Jiaranaikulwanitch, J.; Meepowpan, P.; Daranarong, D.; Srimuang, C.; Topham, P. D.; Punyodom, W. Direct Extraction of Hemp Leaf-Derived Cannabidiol (CBD) and Encapsulation into Biopolymer Nanoparticles for Diffusion-Based Drug Release. *J. Polym. Environ.* **2025**, *33* (9), 4247−4270.
(58) Fissan, H.; Ristig, S.; Kaminski, H.; Asbach, C.; Epple, M. Comparison of different characterization methods for nanoparticle dispersions before and after aerosolization. *Anal. Methods* **2014**, *6* (18), 7324−7334.
(59) Branda, F.; Silvestri, B.; Costantini, A.; Luciani, G. Effect of exposure to growth media on size and surface charge of silica based Stöber nanoparticles: A DLS and ζ-potential study. *J. Sol-Gel Sci. Technol.* **2015**, *73* (1), 54−61.
(60) Zeng, J.; Aigner, A.; Czubayko, F.; Kissel, T.; Wendorff, J. H.; Greiner, A. Poly (vinyl alcohol) nanofibers by electrospinning as a protein delivery system and the retardation of enzyme release by additional polymer coatings. *Biomacromolecules* **2005**, *6* (3), 1484−1488.
(61) Kakade, M. V.; Givens, S.; Gardner, K.; Lee, K. H.; Chase, D. B.; Rabolt, J. F. Electric field induced orientation of polymer chains in macroscopically aligned electrospun polymer nanofibers. *J. Am. Chem. Soc.* **2007**, *129* (10), 2777−2782.
(62) Perfetti, M.; Gallucci, N.; Russo Krauss, I.; Radulescu, A.; Pasini, S.; Holderer, O.; D'Errico, G.; Vitiello, G.; Bianchetti, G. O.; Paduano, L. Revealing the aggregation mechanism, structure, and internal dynamics of poly (vinyl alcohol) microgel prepared through liquid−liquid phase separation. *Macromolecules* **2020**, *53* (3), 852−861.
(63) Atanase, L. I.; Riess, G. Poly (vinyl alcohol-co-vinyl acetate) complex formation with anionic surfactants particle size of nanogels and their disaggregation with sodium dodecyl sulfate. *Colloids Surf., A* **2010**, *355* (1−3), 29−36.
(64) Qin, Z.; Li, Y.; Feng, N.; Fei, X.; Tian, J.; Xu, L.; Wang, Y. Modulating the performance of lipase-hydrogel microspheres in a "micro water environment". *Colloids Surf., B* **2023**, *223*, 113171.
(65) Rodriguez-Abetxuko, A.; Sánchez-DeAlcázar, D.; Muñumer, P.; Beloqui, A. Tunable polymeric scaffolds for enzyme immobilization. *Front. Bioengin. Biotechnol.* **2020**, *8*, 830.
(66) Qi, H.; Yang, L.; Shan, P.; Zhu, S.; Ding, H.; Xue, S.; Wang, Y.; Yuan, X.; Li, P. The stability maintenance of protein drugs in organic coatings based on nanogels. *Pharmaceutics* **2020**, *12* (2), 115.
(67) Sakai, S.; Antoku, K.; Yamaguchi, T.; Kawakami, K. Transesterification by lipase entrapped in electrospun poly (vinyl alcohol) fibers and its application to a flow-through reactor. *J. Biosci. Bioengin.* **2008**, *105* (6), 687−689.

https://doi.org/10.1021/acsomega.5c09274
ACS Omega 2026, 11, 5608−5621

(68) Sakai, S.; Antoku, K.; Yamaguchi, T.; Watanabe, R.; Kawabe, M.; Kawakami, K. Electrospun PVA fibrous mats immobilizing lipase entrapped in alkylsilicate cages: Application to continuous production of fatty acid butyl ester. *J. Mol. Catal. B: Enzym.* **2010**, *63* (1−2), 57−61.
(69) Frizzell, H.; Ohlsen, T. J.; Woodrow, K. A. Protein-loaded emulsion electrospun fibers optimized for bioactivity retention and pH-controlled release for peroral delivery of biologic therapeutics. *Int. J. Pharm.* **2017**, *533* (1), 99−110.

https://doi.org/10.1021/acsomega.5c09274
ACS Omega 2026, 11, 5608−5621